The Astrophysical Journal, 651:93–100, 2006 November 1

A THREE-DIMENSIONAL STUDY OF THE LOCAL ENVIRONMENT OF BRIGHT *IRAS* GALAXIES: THE ACTIVE GALACTIC NUCLEUS–STARBURST CONNECTION

Elias Koulouridis,[1,2] Vahram Chavushyan,[3,4] Manolis Plionis,[1,3]
Yair Krongold,[4] and Deborah Dultzin-Hacyan[4]
Received 2006 May 12; accepted 2006 June 14

ABSTRACT

We present a three-dimensional study of the local ($\leq 100\ h^{-1}$ kpc) and the large scale ($\leq 1\ h^{-1}$ Mpc) environment of bright *IRAS* balaxies (BIRGs). For this purpose we use 87 BIRGs located at high Galactic latitudes (with $0.008 \leq z \leq 0.018$), as well as a control sample of nonactive galaxies having the same morphological, redshift, and diameter size distributions as the corresponding BIRG sample. Using the Center for Astrophysics and the Southern Sky Redshift Survey galaxy catalogs ($m_b \lesssim 15.5$), as well as our own spectroscopic observations ($m_b \lesssim 19.0$), for a subsample of the original BIRG sample, we find that the fraction of BIRGs with a close neighbor is significantly higher than that of their control sample. Comparing with a related analysis of Seyfert 1 and Seyfert 2 galaxies by Koulouridis and coworkers, we find that BIRGs have a similar environment to that of Seyfert 2 galaxies, although the fraction of BIRGs with a bright, close neighbor is even higher than that for Seyfert 2 galaxies. An additional analysis of the relation between FIR colors and the type of activity of each BIRG shows a significant difference between the colors of strongly interacting and noninteracting starbursts and a resemblance between the colors of noninteracting starbursts and Seyfert 2 galaxies. Our results support the view that close interactions can drive molecular clouds toward the galactic center, triggering starburst activity and obscuring the nuclear activity. When the close neighbor moves away, starburst activity is reduced with the simultaneous appearance of an obscured (type 2) active galactic nucleus (AGN). Finally, the complete disentanglement of the pair gives birth to an unobscured (type 1) AGN.

Subject headings: galaxies: active — galaxies: starburst — infrared: galaxies — large-scale structure of universe

Online material: color figures

1. INTRODUCTION

The *IRAS* Revised Bright Galaxy Sample by Sanders et al. (2003) includes all galaxies with total 60 μm flux density greater than 5.24 Jy. The sample is the result of a highly complete flux-limited survey conducted by *IRAS* covering the entire sky at Galactic latitudes $|b| \geq 5^\circ$ and was compiled after the final calibration of the *IRAS* Level 1 Archive. It offers far more accurate and consistent measurements of the flux of objects with extended emission. In addition, the infrared fluxes of over 100 sources from the sample were recalculated by *IRAS* High Resolution (HIRES) processing, which allowed the deconvolution of close galaxy pairs (Surace et al. 2004). The latter provides a database of the *IRAS* galaxies which is more reliable than ever and has proved crucial for statistical studies like this one.

While the relation between ultraluminous infrared galaxies (ULIRGs) and strong interactions has been thoroughly studied (e.g., Sanders et al. 1999; Wang et al. 2006), this is not the case for the environment of moderate- and low-luminosity infrared galaxies. A two-dimensional analysis by Krongold et al. (2002) showed a trend for their bright *IRAS* galaxy (BIRG) sample to have more neighbors than normal and Seyfert 1 galaxies, but to relatively agree with Seyfert 2 galaxies. However, the BIRG population consists of various types of active galaxies, including starbursts (the majority), Seyfert, LINERs, and normal galaxies, and thus it would be of great interest to clarify the connection between infrared emission, interactions, and different types of active galaxies.

During the last decade, many studies have investigated the relation among interacting galaxies, starbursting, and nuclear activity (e.g., Hernández-Toledo et al. 2001; Ho 2005). Despite the plethora of available information, searches for correlations between the above physical processes are inconclusive, the only exception being the coupling between interactions and starbursting. However, there is evidence that AGN galaxies host a poststarburst stellar population (e.g., Boisson et al. 2000; González Delgado et al. 2001), while Kauffmann et al. (2003) showed that the fraction of poststarburst stars increases with AGN emission. Proving a relation of this type between starburst and AGN galaxies would simultaneously also solve the problem of the AGN triggering mechanism; interactions would be the main cause, generated by starbursting and/or the feeding of a central black hole. However, proving this relation is not a trivial task. The main difficulty arises from the fact that the star formation rate (SFR) estimation in AGN host galaxies is still problematic. All SFR estimation methods present complications, and even those based on the FIR continuum are doubtful, since the contribution of the active nuclei is unknown (e.g., Ho 2005).

Despite the difficulties, some studies based on different diagnostics seem to conclude that there is indeed an evolutionary sequence from starburst to type 2 and then to type 1 AGN galaxies (e.g., Oliva et al. 1999; Krongold et al. 2002). In addition, Kim et al. (2006), using the [O II] emission line as a SFR indicator, reached the conclusion that type 2 quasars are the precursors of type 1 quasars, supporting previous claims. These studies are based on the observed differences between different types of AGNs and

[1] Institute of Astronomy and Astrophysics, National Observatory of Athens, I. Metaxa and Vas. Pavlou Streets, Palaia Penteli, 152 36 Athens, Greece.
[2] Physics Department, University of Patras, Panepistimioupolis Patron, 26500 Patras, Greece.
[3] Instituto Nacional de Astrofísica, Optica, y Electrónica, A.P. 51 y 216, C.P. 72000, Puebla, Mexico.
[4] Instituto de Astronomía, Univesidad Nacional Autónoma de México, A.P. 70-264, 04510 México D.F., Mexico.

TABLE 1

OUR BRIGHT *IRAS* SAMPLE GALAXIES THAT RESIDE IN THE SKY REGION COVERED BY THE SSRS AND CfA2 CATALOGS

Name	R.A. (J2000.0)	Decl. (J2000.0)	m_B	z	D (h^{-1} kpc)	Type
NGC 0023	00 09 53.1	25 55 25	12.50	0.0152	Isolated	Starburst
ESO 079-G003	00 14 54.7	−39 11 19	12.50	0.0090	Isolated	Normal
NGC 0174	00 36 59.0	−29 28 40	13.62	0.0116	Isolated	Starburst
UGC 00556	00 54 49.6	29 14 43	15.30	0.0154	Isolated	LINER
UGC 00903	01 21 47.1	17 35 34	14.70	0.0084	Isolated	Unclassified
ESO 353-G020	01 34 51.6	−36 08 08	13.95	0.0161	Isolated	Normal
NGC 0716	01 52 59.3	12 42 31	14.00	0.0152	Isolated	Normal
UGC 01451	01 58 29.9	25 21 34	14.30	0.0164	Isolated	Normal
NGC 0835	02 09 24.5	−10 08 06	13.14	0.0138	11.00	Starburst
NGC 0838	02 09 38.3	−10 08 45	14.22	0.0128	27.82	Starburst
NGC 0839	02 09 42.8	−10 10 59	14.20	0.0128	27.91	Starburst
NGC 0873	02 16 32.2	−11 20 52	12.83	0.0134	Isolated	Starburst
NGC 0877	02 17 58.5	14 32 53	12.50	0.0131	Isolated	Starburst
NGC 0922	02 25 04.4	−24 47 15	12.63	0.0103	Isolated	Starburst
NGC 0992	02 37 25.2	21 06 06	13.50	0.0138	30.32	Starburst
NGC 1083	02 45 40.5	−15 21 24	15.19	0.0137	Isolated	Starburst
NGC 1134	02 53 40.9	13 00 58	13.20	0.0121	77.18	Normal
UGC 02403	02 55 57.2	00 41 36	13.20	0.0139	Isolated	Starburst
NGC 1204	03 04 39.9	−12 20 25	14.21	0.0143	Isolated	Starburst
ESO 420-G013	04 13 49.5	−32 00 23	13.52	0.0121	Isolated	Seyfert 2
NGC 1614	04 31 35.5	−08 40 56	12.00	0.0160	2.00	Starburst
NGC 2782	09 14 05.5	40 06 54	12.66	0.0085	Isolated	Starburst
NGC 1667	04 46 10.5	−06 24 24	13.00	0.0150	Isolated	Seyfert 2
NGC 2785	09 15 15.8	40 55 08	14.90	0.0088	52.00	Starburst
NGC 2856	09 24 16.9	49 14 58	13.90	0.0088	26.53	Starburst
NGC 3147	10 16 55.8	73 24 07	11.52	0.0094	Isolated	Seyfert 2
NGC 3221	10 22 21.0	21 34 12	14.30	0.0137	Isolated	Normal
NGC 3367	10 46 34.5	13 45 10	12.22	0.0101	Isolated	Unclassified
NGC 3508	11 02 59.6	−16 17 17	13.20	0.0130	Isolated	Starburst
*NGC 3690	11 28 32.9	58 33 19	13.20	0.0104	2.16	Starburst
NGC 3735	11 36 01.0	70 32 06	12.60	0.0090	Isolated	Seyfert 2
NGC 3994	11 57 37.0	32 16 39	13.68	0.0105	18.17	LINER
NGC 3995	11 57 44.9	32 17 42	12.96	0.0109	18.65	Starburst
NGC 4175	12 12 30.7	29 10 10	14.20	0.0131	17.39	Seyfert 2
NGC 4194	12 14 10.1	54 31 34	13.00	0.0084	Isolated	Starburst
NGC 4332	12 22 47.8	65 50 36	13.20	0.0091	Isolated	Starburst
NGC 4388	12 25 46.7	12 39 40	12.20	0.0084	Isolated	Seyfert 2
NGC 4433	12 27 38.6	−08 16 49	12.90	0.0099	63.09	Normal
MCG 02-33-098	13 02 19.8	−15 46 07	15.38	0.0159	Isolated	Starburst
MCG 03-34-014	13 12 34.5	−17 32 28	13.02	0.0092	Isolated	Normal
NGC 5020	13 12 40.1	12 35 57	13.40	0.0112	Isolated	Normal
IC 0860	13 15 03.7	24 37 05	14.80	0.0129	Isolated	Unclassified
NGC 5073	13 19 21.4	−14 51 46	13.50	0.0091	Isolated	Starburst
IC 4280	13 32 53.0	−24 12 29	13.51	0.0163	93.52	Starburst
NGC 5371	13 55 40.3	40 27 38	11.59	0.0085	Isolated	Unclassified
NGC 5394	13 58 33.7	37 27 10	13.85	0.0116	19.44	Starburst
NGC 5395	13 58 37.9	37 25 27	12.47	0.0116	19.10	LINER
NGC 5430	14 00 45.7	59 19 46	13.08	0.0099	Isolated	Starburst
NGC 5433	14 02 36.1	32 30 35	14.00	0.0145	Isolated	Starburst
NGC 5427	14 03 25.7	−06 01 53	11.93	0.0087	22.81	Seyfert 2
NGC 5595	14 24 13.2	−16 43 28	13.12	0.0090	32.63	Normal
NGC 5597	14 24 27.2	−16 45 50	13.32	0.0089	32.68	Starburst
NGC 5653	14 30 10.3	31 12 50	13.39	0.0119	Isolated	Starburst
NGC 5728	14 42 23.6	−17 15 14	12.81	0.0095	Isolated	Seyfert 2
NGC 5757	14 47 46.2	−19 04 45	13.50	0.0089	Isolated	Starburst
NGC 5793	14 59 24.6	−16 41 38	14.17	0.0117	37.36	Seyfert 2
UGC 09668	14 55 56.0	83 31 29	13.80	0.0131	63.55	Starburst
CGCG 049-057	15 13 13.2	07 13 26	15.50	0.0130	Isolated	Starburst
NGC 5900	15 15 05.0	42 12 28	15.00	0.0084	70.48	Normal
NGC 5930	15 26 07.8	41 40 30	13.00	0.0087	3.59	Starburst
NGC 5936	15 30 01.1	12 59 21	13.41	0.0134	Isolated	Starburst
NGC 5937	15 30 46.0	−02 49 49	13.35	0.0095	Isolated	Starburst
NGC 5990	15 46 16.0	02 24 49	13.10	0.0128	84.90	Seyfert 2
*NGC 6052	16 05 13.1	20 32 27	14.70	0.0151	Isolated	Starburst

TABLE 1—*Continued*

Name	R.A. (J2000.0)	Decl. (J2000.0)	m_B	z	D (h^{-1} kpc)	Type
ESO 402-G026	21 22 31.7	−36 40 57	13.69	0.0093	Isolated	Normal
NGC 7130	21 48 19.5	−34 57 10	13.33	0.0161	Isolated	Unclassified
NGC 7172	22 02 02.2	−31 52 15	12.95	0.0086	46.75	Seyfert 2
IC 5179	22 16 09.3	−36 50 43	12.46	0.0114	Isolated	Starburst
ESO 534-G009	22 38 41.7	−25 51 02	13.55	0.0113	86.40	LINER
NGC 7469	23 03 15.5	08 52 24	13.00	0.0162	18.76	Unclassified
NGC 7541	23 14 43.0	04 32 03	12.70	0.0089	23.62	Starburst
NGC 7591	23 18 16.0	06 35 08	13.80	0.0165	Isolated	Seyfert 2
NGC 7678	23 28 27.7	22 25 15	12.70	0.0116	Isolated	Seyfert 2
NGC 7714	23 36 14.0	02 09 17	13.10	0.0093	16.12	Starburst
NGC 7769	23 51 04.7	20 09 03	13.10	0.0141	2.64	Unclassified
NGC 7771	23 51 24.7	20 06 41	13.39	0.0143	13.23	Unclassified
UGC 12914	24 01 38.0	23 29 04	13.20	0.0146	14.82	Unclassified
UGC 12195	24 01 42.2	23 29 41	13.90	0.0145	14.33	Unclassified

NOTE.—Units of right ascension are hours, minutes, and seconds, and units of declination are degrees, arcminutes, and arcseconds.

the resemblance of type 2 objects to starbursts. This raises doubts about the simplest version of the unification scheme of AGNs. It is true that the recent discovery of 10 μm silicate emission in two luminous quasars implies the presence of dust, but it is not yet clear what the spatial distribution of this material is (Siebenmorgen et al. 2005). In addition, silicate emission is not yet detected in other type 1 objects, and thus more observations are needed to establish the existence of dusty tori.

We can summarize all the previous discussion in two statements: (1) the AGN-starburst connection is still not well established, and (2) the AGN unification model, although successful in interpreting many observational facts, remains fragile. From our point of view, our BIRG sample offers a homogeneous and complete database, which is ideal for a statistical study of these issues.

We discuss our galaxy samples in § 2. Our data analysis and results are presented in § 3, while in § 4 we discuss our results and present our conclusions. Due to the fact that all of our samples are local, cosmological corrections of galaxy distances are negligible. Throughout our paper we use $H_0 = 100\ h$ km s^{-1} Mpc^{-1}.

2. OBSERVATIONS AND SAMPLES

2.1. *BIRG Galaxies and Control Sample*

The bright *IRAS* sample consists of 87 objects with redshifts between 0.008 and 0.018 and was compiled from the BIRG survey by Soifer et al. (1989) for the Northern Hemisphere and by Sanders et al. (1995) for the Southern. It includes only high Galactic latitude objects ($|b| > 30^\circ$) in order to avoid extinction and confusion with Galactic stars. All objects lay in the luminosity range of $10^{10}\ h^{-2}\ L_\odot \leq L_{\rm FIR} \leq 10^{12}\ h^{-2}\ L_\odot$. This sample is volume limited, and a $V/V_{\rm max}$ test gives a value of 0.47 ± 0.05. Since the BIRG survey is highly complete, this sample is expected to be as well. More details about the sample selection are given in Krongold et al. (2002). In addition, we have refined the bright *IRAS* sample by correcting the infrared fluxes using "The *IRAS* Revised Bright Galaxy Sample" by Sanders et al. (2003). Furthermore, for interacting galaxies we used the corrected fluxes given by Surace et al. (2004).

We also use the control sample compiled by Krongold et al. (2002) in such a way as to reproduce the main characteristics, other than the infrared emission, of the bright *IRAS* sample. Specifically, the control sample was compiled from the original CfA catalog to closely reproduce the redshift, morphological type, and diameter size distributions of the corresponding *IRAS* sample. In other words, the selection of the *IRAS* sample and its corresponding control sample is exactly the same, the only difference being the infrared luminosity. This is very important in order to validate that any possible environmental effect is related to the mechanisms that produce the observed high-infrared luminosity and not to possible differences in the host galaxies or sample biases.

In Table 1 we present the names, celestial coordinates, Zwicky magnitudes, redshifts, nearest neighbor projected linear distance, and spectral types of our final list of BIRGs.

2.2. *The Southern Sky Redshift Survey and the Center for Astrophysics 2 Catalogs*

In order to investigate the local and large scale environment around our BIRG and control sample galaxies, we use the Center for Astrophysics (CfA2) and the Southern Sky Redshift Survey (SSRS) galaxy catalogs, which cover a large solid angle of the sky. Although these galaxy catalogs date from the 1980s and 1990s, they still provide an important database for studies of the properties of galaxies and their large-scale distribution in the nearby universe. We briefly present the main characteristics of these catalogs.

The CfA2 redshift catalog contains approximately 18,000 galaxy redshifts in the northern sky down to a magnitude limit of $m_B = 15.5$ (Huchra 1990). The magnitude system used is the merging of the original Zwicky magnitudes and the more accurate RC1 $B(0)$ magnitudes. These exhibit a scatter of $\sim$0.3 mag (e.g., Bothun & Cornell 1990). Following Huchra (1990), we do not attempt to translate these magnitudes to a standard photometric system since this requires accurate knowledge of the morphological type and size of each individual galaxy.

The SSRS catalog (da Costa et al. 1998) contains redshifts, B magnitudes, and morphological classifications for $\sim$5400 galaxies in two regions covering a total of 1.70 sr in the Southern Celestial Hemisphere, and it is more than 99% complete down to $m_B = 15.5$. The galaxies have positions accurate to about 1″ and magnitudes with an rms scatter of about 0.3 mag. The radial velocity precision is $\sim$40 km s^{-1}.

Note that in the regions covered by the SSRS and CfA2 catalogs only a subsample of the original BIRGs and their control samples can be found (76 BIRGs and 61 control galaxies). In order to test whether these subsamples are statistically equivalent with their parent samples (i.e., their diameter, morphological type, and redshift distributions) we used the Kolmogorov-Smirnov (K-S) two-sample test. We verified that the null hypothesis, the subsamples

TABLE 2

SUBSAMPLE OF BIRG GALAXIES IN OUR SPECTROSCOPIC SURVEY

Name	R.A. (J2000.0)	Decl. (J2000.0)	O_{MAPS} Integrated	z	Type
NGC 0023	00 09 53.1	25 55 25	13.95	0.0152	Starburst
None					
UGC 00556	00 54 49.6	29 14 43	15.63	0.0154	LINER
Neighbor 1	00 54 51.1	29 16 25	17.03	0.0152 ± 0.0002	
NGC 0716	01 52 59.3	12 42 31	14.51	0.0152	Normal
None					
UGC 01451	01 58 29.9	25 21 34	15.41	0.0164	Normal
None					
NGC 0835	02 09 24.5	−10 08 06	13.67[a]	0.0138	Starburst
Neighbor 1	02 09 20.9	−10 08 00	[a]	0.0130 ± 0.0002	
Neighbor 2	02 09 38.3	−10 08 45	14.89	0.0133 ± 0.0004	
Neighbor 3	02 09 42.8	−10 10 59	15.01	0.0132 ± 0.0004	
NGC 0877	02 17 58.5	14 32 53	13.07	0.0131	Starburst
Neighbor 1	02 17 53.3	14 31 17	16.04	0.0136 ± 0.0007	
Neighbor 2	02 17 26.3	14 34 49	16.77	0.013376[b]	
NGC 0922	02 25 04.4	−24 47 15	13.25	0.0103	Starburst
Neighbor 1	02 24 30.0	−24 44 44	16.73	0.1054[b]	
NGC 0992	02 37 25.2	21 06 06	15.39	0.0138	Starburst
Neighbor 1	02 37 28.2	21 08 31	16.99	0.0126 ± 0.0004	
NGC 1614	04 31 35.5	−08 40 56	14.55	0.0160	Seyfert 2
Neighbor 1	04 31 35.5	−08 40 56	16.44	0.0160	
NGC 1667	04 46 10.5	−06 24 24	13.00[c]	0.0160	Seyfert 2
None					
UGC 02403	02 55 57.2	00 41 36	15.33	0.0139	Starburst
Neighbor 1	02 55 58.9	00 40 26	19.10	0.0749 ± 0.0002	
NGC 2785	09 15 15.8	40 55 08	14.85	0.0088	Starburst
Neighbor 1	09 15 33.8	40 55 27	14.54	0.0653 ± 0.0004	
Neighbor 2	09 14 43.1	40 52 47	14.54	0.008319[b]	
Neighbor 3	09 14 35.6	40 55 24	17.58	0.008933[b]	
NGC 2856	09 24 16.9	49 14 58	14.71	0.0088	Starburst
Neighbor 1	09 24 03.1	49 12 16	14.52	0.0089 ± 0.0004	
NGC 3221	10 22 21.0	21 34 12	13.87	0.0137	Normal
Neighbor 1	10 22 26.0	21 32 31	17.06	0.0117 ± 0.0004	
Neighbor 2	10 22 21.1	21 31 00	17.89	0.0539 ± 0.0003	
Neighbor 3	10 22 13.4	21 30 42	18.67	0.0128 ± 0.0007	
NGC 3690	11 28 32.9	58 33 19	13.76[a]	0.0104	Starburst
Neighbor 1	11 28 33.5	58 33 47	[a]	0.010411[b]	
Neighbor 2	11 28 27.3	58 34 42	[a]	0.0132 ± 0.0001	
Neighbor 3	11 28 45.8	58 35 36	16.14	0.0604 ± 0.0002	
NGC 4388	12 25 46.7	12 39 40	12.79	0.0084	Seyfert 2
Neighbor 1	12 25 41.7	12 48 38	14.50	0.0021 ± 0.0001	
Neighbor 2	12 25 15.2	12 42 53	15.87	<0.001[b]	
IC 0860	13 15 03.7	24 37 05	15.31	0.0129	Unclassified
None					
NGC 5073	13 19 21.4	−14 51 46	14.03	0.0091	Starburst
Neighbor 1	13 19 34.1	−14 46 22	16.21	0.0350 ± 0.0006	
Neighbor 2	13 18 56.4	−14 54 13	16.41	0.0347 ± 0.0001	
NGC 5433	14 02 36.1	32 30 35	14.68	0.0145	Starburst
Neighbor 1	14 02 39.0	32 27 50	18.00	0.0142 ± 0.0008	
Neighbor 2	14 02 20.5	32 26 53	16.17	0.00141 ± 0.0007	
NGC 5653	14 30 10.3	31 12 50	14.10	0.0119	Starburst
None					
NGC 5990	15 46 16.0	02 24 49	14.29	0.0128	Starburst
Neighbor 1	15 46 28.9	02 23 09	18.16	0.0468 ± 0.0002	
Neighbor 2	15 46 23.2	02 21 34	17.58	0.0480 ± 0.0003	
Neighbor 3	15 45 45.9	02 24 35	15.87	0.0141 ± 0.0001	
NGC 7541	23 14 43.0	04 32 03	13.22	0.0089	Starburst
Neighbor 1	23 14 34.5	04 29 54	14.70	0.0080 ± 0.0006	

TABLE 2—*Continued*

Name	R.A. (J2000.0)	Decl. (J2000.0)	O_{MAPS} Integrated	z	Type
NGC 7714	23 36 14.0	02 09 17	13.10[c]	0.0093	Starburst
Neighbor 1	23 36 22.1	02 09 24	14.90[c]	0.0089 ± 0.0001	
NGC 7771	23 51 24.7	20 06 41	13.81[a]	0.0143	Unclassified
Neighbor 1	23 51 22.5	20 05 47	[a]	0.0145 ± 0.0008	
Neighbor 2	23 51 13.1	20 06 12	17.13	0.013679[b]	
Neighbor 3	23 51 04.0	20 09 02	14.05	0.0139 ± 0.0003	
Neighbor 4	23 51 13.9	20 13 46	17.02	0.043527[b]	

NOTE.—. Below each BIRG, we list all its neighbors within a projected distance of 100 h^{-1} kpc with their measured redshifts. Units of right ascension are hours, minutes, and seconds, and units of declination are degrees, arcminutes, and arcseconds.

[a] Unresolved neighboring galaxies.

[b] Redshift from NED.

[c] Zwicky blue magnitude (region not covered by MAPS catalog).

being equivalent with their parent samples, cannot be rejected at any significant statistical level.

2.3. *Our Spectroscopic Observations*

In order to cover a larger magnitude difference between the BIRGs and their nearest neighbor than that imposed by the CFA2/SSRS magnitude limit ($m_B \sim 15.5$), we have obtained our own spectroscopic observations of fainter neighbors around a subsample of our BIRGs consisting of 24 galaxies (selected randomly from their parent sample). Around each BIRG we have obtained spectra of all neighboring galaxies within a projected radius of 100 h^{-1} kpc and a magnitude limit of $m_B \lesssim 19.0$.

Our aim with this new, fainter neighbor search is not to establish or disprove the existence of close neighbors around the BIRGs. This is done by using the brighter SSRS and CfA2 catalogs, at the magnitude limit of which we have well-defined control samples. What we seek with these observations is to facilitate a comparison with a similar analysis of Seyfert galaxies by Koulouridis et al. (2006) in which Seyfert 2s were found to have a significantly higher fraction of neighbors with respect to Seyfert 1s. In other words, we wish to establish whether the fractional differences between the Seyfert 1, Seyfert 2, and BIRG samples of galaxies, already determined (or not) as significant with respect to their control samples, continue to fainter magnitudes.

Optical spectroscopy was carried out using the Landessternwarte Faint Object Spectrograph and Camera (LFOSC; Zickgraf et al. 1997) mounted on the 2.1 m Guillermo Haro telescope in Cananea, operated by the National Institute of Astrophysics, Optics, and Electronics of Mexico. A setup covering the spectral range 4200–9000 Å with a dispersion of 8.2 Å pixel^{-1} was adopted. The effective instrumental spectral resolution was about 18 Å. The data reduction was done using the IRAF packages and included bias and flat-field corrections, cosmic-ray cleaning, wavelength linearization, and flux transformation.

In Table 2 we present the BIRG name, coordinates, redshift, and magnitude for this subsample of BIRGs. Below the row of each BIRG, we list the corresponding data for all its neighbors, within a projected separation of 100 h^{-1} kpc. Since Zwicky magnitudes were not available for the fainter neighbors and in order to provide a homogeneous magnitude system for all the galaxies, we decided to list the O_{MAPS} magnitudes[5] for all galaxies in Table 2.[6] The neighbor-measured redshift is presented in the fifth column (in some very few cases we list the redshift from the NASA/IPAC Extragalactic Database). The uncertainties listed are estimated from the redshift differences that result from using different emission lines.

[5] *O* (blue) POSS I plate magnitudes of the Minnesota Automated Plate Scanner (MAPS) system.

[6] See http://aps.umn.edu/docs/photometry.

3. ANALYSIS AND RESULTS

We search for the nearest neighbor around each BIRG and control galaxy in our samples with the aim of estimating the fraction of BIRG and normal galaxies that have a close neighbor. To define the neighborhood search we use two parameters, the projected linear distance (D) and the radial velocity separation (δv) between the central BIRG and the neighboring galaxies found in the CfA2 and SSRS catalogs or in our own spectroscopic observations. We search for neighbors with $\delta v \leq 600$ km s^{-1}, which is roughly the mean galaxy pairwise velocity of the CfA2 and SSRS galaxies or about twice the mean pairwise galaxy velocity when clusters of galaxies are excluded (Marzke et al. 1994). Note, however, that our results remain robust even for $\delta v \leq 1000$ km s^{-1}. We then define the fraction of BIRG and normal galaxies that have their nearest neighbor within the selected δv separation as a function of increasing D.

3.1. *Neighbors with $m_B \lesssim 15.5$ (CfA2 and SSRS)*

In Figure 1 (*top panels*) we plot the fraction of BIRG and control galaxies as a function of the projected distance (D) of the first companion and for two velocity separations ($\delta v \leq 200$ and ≤ 600 km s^{-1}). For comparison, we also plot the results of a similar analysis by Koulouridis et al. (2006) concerning Seyfert galaxies and their control samples.

It is evident that a significantly higher fraction of BIRG galaxies have a near neighbor within $D \lesssim 100\ h^{-1}$ kpc with respect to their control sample. In Koulouridis et al. (2006) we found that there is a significantly higher fraction of Seyfert 2 galaxies (∼27%) having a near neighbor within $D \lesssim 75\ h^{-1}$ kpc with respect to both their control sample and the Seyfert 1 galaxies (∼14%). Adding here the BIRG sample, which includes mostly starburst and Seyfert 2 galaxies (see Table 1), we can clearly see that an even higher fraction of BIRGs (∼42%) tend to have a close companion within $D \lesssim 75\ h^{-1}$ kpc. The latter needs a further explanation, since it is not consistent with most AGN-starburst connection scenarios, which suggest a simultaneous creation of starburst and Seyfert 2 nuclei triggered by interactions.

In order to investigate whether fainter neighbors than those found in the relatively shallow CFA2 and SSRS catalogs exist around our BIRGs, we have performed a spectroscopic survey of all neighbors with $m_B \lesssim 19.0$ ($\gtrsim 3$ mag fainter than the CfA2 and SSRS limits). This limit translates into an absolute magnitude limit of $M_B \sim -15.2$ for the most distant objects in our sample

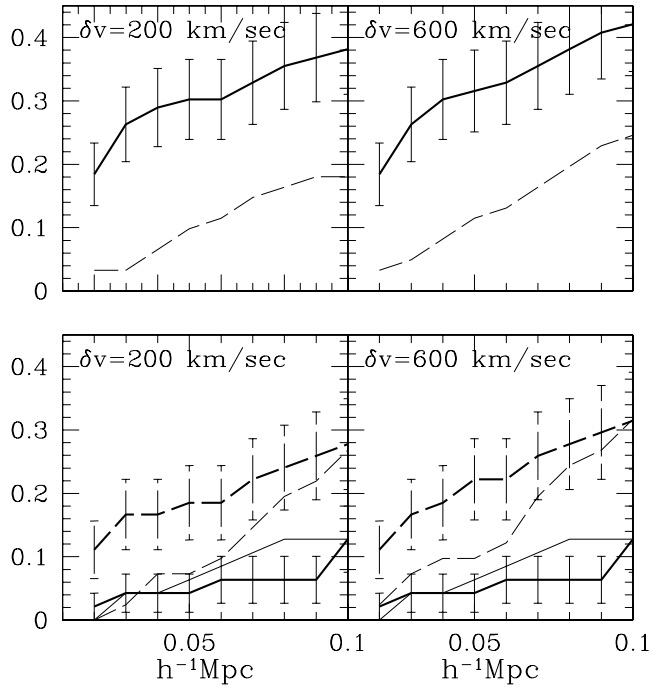

FIG. 1.—*Top panels:* Fraction of BIRGs (*thick line*) and their control sample galaxies (*thin dashed line*) that have their nearest neighbor within the indicated redshift separation, as a function of projected distance. *Bottom panels:* Corresponding Seyfert 1 (*dashed lines*) and Seyfert 2 (*solid lines*) fractions by Koulouridis et al. (2006). [*See the electronic edition of the Journal for a color version of this figure*.]

($z = 0.018$). This magnitude is even fainter than that of the Small Magellanic Cloud.

3.2. *Neighbors with* $m_B \lesssim 19.0$ (*Our Spectroscopy*)

Here we present results of our spectroscopic observations of all the neighbors with $D \leq 75\ h^{-1}$ kpc and $m_B \lesssim 19.0$ for the subsample of 24 BIRGs (see Table 2). We find that in total, 13 out of the 24 BIRGs have at least one close neighbor within the above limits, with nine of these having neighbors already detected in the SSRS and CfA2 catalogs; i.e., only four BIRGs have neighbors fainter than $m_b \sim 15.5$. This implies that the fraction of BIRGs having a close neighbor (within $D \leq 75\ h^{-1}$ kpc and for $\delta v \leq 600$ km s^{-1}) increases only by ~45% when going fainter.

Koulouridis et al. (2006) showed that the percentage of both Seyfert 1 and Seyfert 2 galaxies that have a close neighbor (within the above limits) increases correspondingly by about 100% when descending from $m_B \lesssim 15.5$ to $m_B \lesssim 19.0$ (but remember that the host galaxies have magnitudes slightly closer to the CFA2 and SSRS limit). In detail, while the percentage of Seyfert 1 and Seyfert 2 galaxies having a close neighbor increases from 14% to 27% and from 27% to 55%, respectively, for BIRGs it increases from 42% to 54%, reaching the equivalent Seyfert 2 levels. We summarize that BIRGs, with respect to their control sample, show an excess of close neighbors, which therefore should be responsible for their excess FIR emission. These results confirm a previous two-dimensional analysis by Krongold et al. (2002) of the same BIRG sample.

Since the fractions of both BIRGs and Seyfert 2 galaxies that have a close neighbor is roughly the same, an interesting question is whether there are any magnitude differences between hosts and neighbors for the BIRGs and the Seyfert 2 galaxies. In Figure 2 we present the distribution of such magnitude differences (Δm) between hosts and the nearest neighbor for the BIRGs and the Seyfert 2 galaxies. Although there appears to be a slight preference for brighter neighbors of the BIRGs with respect to the Seyfert 2 galaxies, the two distributions are statistically equivalent, as quantified by a K-S test that gives a probability of them being drawn from the same parent population of ~0.75.

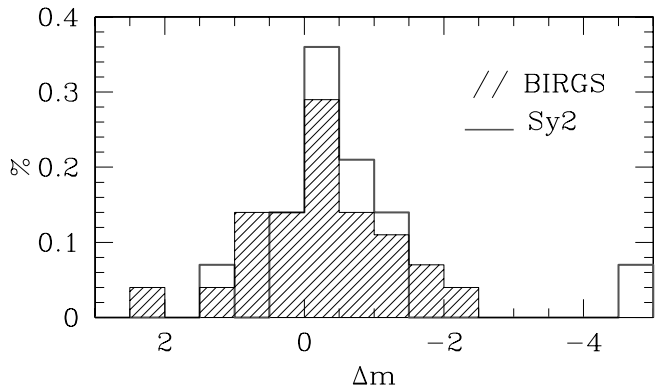

FIG. 2.—Frequency distribution of host (BIRG or Seyfert 2) nearest neighbor magnitude differences. [*See the electronic edition of the Journal for a color version of this figure*.]

3.3. *Large-Scale Environmental Analysis*

Here we investigate whether there are differences in the large-scale environment of BIRGs with respect to their control galaxies and to the Seyfert 1 and Seyfert 2 samples of Koulouridis et al. (2006). To this end we determine the galaxy overdensity, based on the CfA2 and SSRS catalogs, in a region around each BIRG or control sample galaxy. We count all neighboring galaxies around each galaxy within a projected radius of 1 h^{-1} Mpc, and to take into account the galaxy peculiar velocities, we use a radial velocity separation of $\delta v \leq 1000$ km s^{-1}.

We estimate the expected CfA2 and SSRS field galaxy density, $\langle\rho\rangle$, at the distance of each galaxy by integrating the corresponding CfA2 or SSRS luminosity function (Marzke et al. 1994; da Costa et al. 1994), using as a lower integration limit the minimum galaxy luminosity that corresponds to the galaxy catalog magnitude limit (i.e., $m_B = 15.5$) at that distance. We then compute the local overdensity around each AGN, within the previously mentioned cylinder, which is given by $\Delta\rho = (\rho - \langle\rho\rangle)/\langle\rho\rangle$, where $\rho = N/V$ with N the number of neighbors and V the corresponding volume of the cylinder.

In Figure 3 we plot the overdensity frequency distribution for the BIRGs (*left*) and the corresponding distribution of their

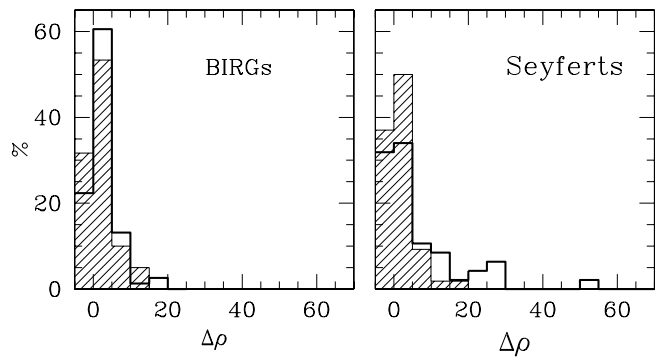

FIG. 3.—*Left:* Frequency distribution of galaxy overdensities around BIRGs (*solid line*) and the control sample (*hatched histogram*). *Right:* Corresponding distribution around Seyfert 1 (*solid line*) and Seyfert 2 (*hatched histogram*) galaxies. Note that here we do not present the corresponding distributions of their control samples (to this end see Koulouridis et al. 2006). [*See the electronic edition of the Journal for a color version of this figure*.]

control galaxy sample. For comparison, we also plot the distributions for the Seyfert galaxies of Koulouridis et al. (2006). A K-S test shows that there is no statistically significant difference between any active galaxy sample (BIRG or Seyfert) and their respective control sample distribution.

However, there is a statistically significant difference at a 0.03 and 0.09 level between the overdensity distributions of BIRGs and Seyfert 1 galaxies, and Seyfert 1 galaxies and Seyfert 2 galaxies, respectively. Similar differences are also found between their respective control samples. On the other hand, the corresponding distributions of BIRGs and Seyfert 2 galaxies (and of their control samples) are statistically equivalent at a 0.9 level. This implies that the large-scale environment of BIRGs and Seyfert 2 galaxies is similar, but significantly different from that of Seyfert 1 galaxies, a difference, which, since it is also seen in their corresponding control samples, should be attributed to differences of the host galaxies. Indeed, Seyfert 1 hosts are earlier type galaxies (e.g., Hunt & Malkan 1999; Koulouridis et al. 2006), which are known to be more clustered than late types (e.g., Willmer et al. 1998).

3.4. *FIR Color Analysis*

In this section we investigate whether there is a relation between the strength of the interaction of BIRGs with their closest neighbor and their FIR characteristics. The strength of any interaction could be parameterized as a function of the distance between the BIRG and its first neighbor. At this first-order analysis, we do not take into account the magnitude difference between BIRGs and their close neighbor, which as we have shown previously (see Fig. 2) does not appear to be significantly different from that of Seyfert 2 galaxies.

We divided the interactions in our sample into three categories based on the proximity of the first neighbor. We consider strong interactions when $D \leq 30\ h^{-1}$ kpc, weak interactions when $30\ h^{-1}$ kpc $\leq D \leq 100\ h^{-1}$ kpc, and no interaction when $D > 100\ h^{-1}$ kpc.

In Figure 4 we present the color-color diagram of $\alpha(60, 25)$ versus $\alpha(25, 12)$, where $\alpha(\lambda_1, \lambda_2)$ is the spectral index defined as $\alpha(\lambda_1, \lambda_2) = \log(S_{\lambda_1}/S_{\lambda_2})/(\lambda_2/\lambda_1)$ with S_{λ_1} the flux in janskys at wavelength λ_1. We can clearly see the differences between the FIR characteristics among different types of galaxies and different interaction strengths. The different interaction strengths are coded by different types of symbols, while the different activity is color coded as indicated in the caption of the figure. We cross-identified classifications of each BIRG, combining various studies such as those of Coziol et al. (1998), Veilleux et al. (1997), Ho et al. (1995), Corbett et al. (2003), de Grijp et al. (1987) and, when available, SDSS spectroscopic data.

It is evident that the FIR characteristics of starburst galaxies in our BIRG sample differ significantly depending on the strength of the interaction. The majority of highly interacting starbursts have $\alpha(60, 25)$ spectral indices greater than -2, while all noninteracting starbursts except one have less. We also find that normal galaxies and LINERs are at the lower end of this sequence. The only highly interacting starburst galaxy below $\alpha(60, 25) = -2.15$ is NGC 7541, which happens to have more than 2 times the typical molecular gas mass of BIRGs (Mirabel & Sanders 1988). The difference between highly interacting and noninteracting starburst galaxies, as quantified by a K-S test, is significant at a >99.9% level when comparing their $\alpha(60, 25)$ index distribution. However, Seyfert 2 galaxies, interacting or not, seem to lay in the same area $[-2.5 < \alpha(60, 25) < -2]$ as noninteracting starburst galaxies, delineated in Figure 4 by blue, dashed lines.

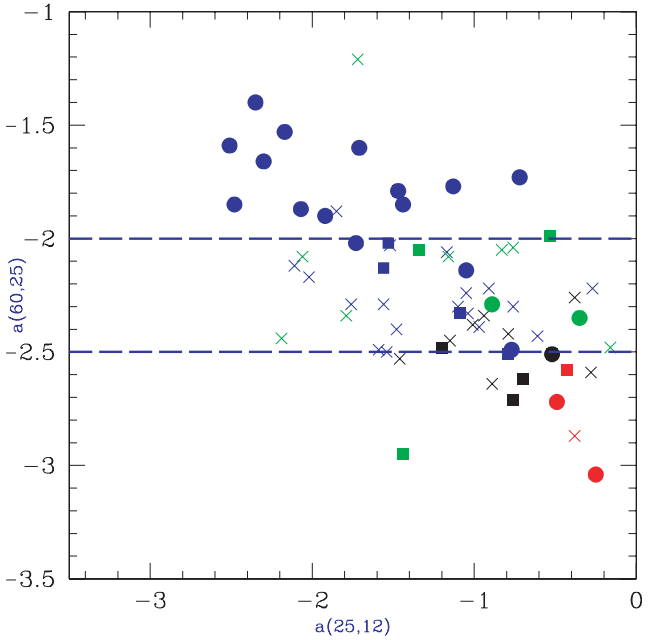

FIG. 4.—FIR color-color diagram: $\alpha(60, 25)$ vs. $\alpha(25, 12)$. The color coding is such that starbursts are represented by blue, Seyfert 2 galaxies by green, LINERs by red, and normal galaxies by black. Highly interacting BIRGs are represented by filled circles, weakly interacting by filled squares, and noninteracting by crosses.

The FIR color analysis of our sample strengthens our previous results. It clearly shows that the starburst activity is higher when interactions are stronger and ceases when the interacting, neighboring galaxy moves away. While the starburst activity weakens (if we link position on the plot with time) Seyfert 2 nuclei appear, giving further evidence on the causal bridging between these objects.

4. DISCUSSION AND CONCLUSIONS

We have compared the three-dimensional environment of a sample of local BIRGs with that of a well-defined control sample, selected in such a way as to reproduce the redshift, morphological type, and diameter size distributions of the BIRG sample. We searched for close neighbors around each BIRG and control sample galaxy using the distribution of CfA2 and SSRS galaxy catalogs, as well as our own spectroscopic observations reaching a fainter magnitude limit (but for a restricted BIRG subsample). We also compared our results with those of a similar analysis of Seyfert galaxies (Dultzin-Hacyan et al. 1999; Koulouridis et al. 2006).

We find that the fraction of BIRG galaxies having a close neighbor, within a projected separation of $75\ h^{-1}$ kpc and a radial velocity difference of $\delta v \leq 600$ km s^{-1}, is significantly higher than the corresponding fraction of its control sample and that of Seyfert 1 galaxies, while it is comparable to that of Seyfert 2 galaxies. This result is in accordance with some previous two-dimensional studies (e.g., Krongold et al. 2002). We reach similar results regarding the large-scale environment of BIRGs (within a projected radial separation of $1\ h^{-1}$ Mpc and a radial velocity difference $\delta v \leq 1000$ km s^{-1}). Once more their behavior resembles that of Seyfert 2s but not of Seyfert 1s. We also find a statistically significant difference between highly interacting and noninteracting BIRGs based on their FIR color properties. Seyfert 2 galaxies appear to display a similar behavior to that of noninteracting starburst galaxies, introducing new evidence for the AGN-starburst connection scenarios.

Our results can be accommodated in a simple evolutionary scenario, starting with an interaction and ending in a Seyfert 1 phase. First, close interactions would drive molecular clouds toward the central area, creating a circumnuclear starburst. Then material could fall even further into the innermost regions of the galaxy, feeding the black hole and giving birth to an AGN, which at first would not be observed due to obscuration. At this stage, only a starburst would be observed. As starburst activity relaxed and obscuration decreased, a Seyfert 2 nucleus would be revealed (still obscured by the molecular clouds from all viewing angles). As a final stage, a Seyfert 1 phase could appear. In this case, the molecular clouds, initially in a spheroidal distribution, could flatten and form a "torus" (as in the unification scheme for Seyfert galaxies). As more material is accreted, it is possible that the AGN strengthens, driving away most of the obscuring clouds, and leaving a "naked" Seyfert 1 nuclei.

If indeed interactions play a role in triggering activity, as suggested by the above picture, then the lack of close companions among Seyfert 1 galaxies implies that the time needed for type 1 activity to appear should be larger than the timescale for an unbound companion to escape from the close environment or comparable to the timescale needed for an evolved merger ($\sim 10^9$ yr; see Krongold et al. 2002).

It should be noted that the evolutionary scenario does not contradict the unification scheme. It implies that Seyfert 1 galaxies and Seyfert 2 galaxies are the same objects (as the unification model proposes) but not necessarily at the same evolutionary phase. However, there could be a phase in which only orientation determines whether an object appears as a Seyfert 1 or a Seyfert 2, which is the stage where molecular clouds form a torus but have not yet been swept away yet.

Evidently, more detailed observations of large samples of galaxies are needed to resolve this important issue. However, such a picture is consistent with the evolutionary scenario suggested by Tran (2003). He studied a sample of Seyfert 2 galaxies in polarized light and found that only 50% of them showed the presence of a hidden broad-line region (HBLR). He suggested that non-HBLR Seyfert 2 galaxies could evolve into HBLR Seyfert 2 galaxies. In this case, the appearance of the BLR could be related to the accretion rate (e.g., Nicastro 2000), and thus to the evolutionary stage of the object. The trend is also consistent with the finding that 50% of Seyfert 2 galaxies also show the presence of a strong starburst (Gu et al. 2001; Cid-Fernandez et al. 2001).

On the brightest end, there is also growing evidence showing that (1) ULIRGs can be the precursors of quasars and (2) ULIRGS are found in very strong interacting systems or in mergers (e.g., Sanders et al. 1999; Wang et al. 2006). Therefore, the evolutionary sequence proposed above could be generalized to all nuclear activity and independent of luminosity (we note that Krongold et al. [2003] suggested a similar scheme for LINERs, which can be considered as the very low luminosity extension of the evolutionary model suggested here). Further evidence comes from the fact that type 2 quasars also tend to be in interaction more often than type 1 quasars (Serber et al. 2006).

In order to better understand the role of interactions in driving starburst and nuclear activity (and the validity of the evolutionary trend), we are in the process of studying AGNs and starburst manifestations in the nearest neighbors of the active galaxies in our samples, since the same physical processes should act on both members of the pair (host and nearest neighbor).

E. K. thanks the Instituto de Astronomía, Universidad Nacional Autónoma de México (IA-UNAM), where a major part of this work was completed, for its warm hospitality. M. P. acknowledges funding by Mexican government research grant CONACyT 39679, V. C. by the CONACyT research grants 39560-F and 42609, and D. D.-H. support from grant IN100703 from DGAPA, PAPIIT, and UNAM. This research has made use of the MAPS catalog of POSS I supported by the University of Minnesota[7] and of the USNOFS Image and Catalogue Archive operated by the United States Naval Observatory, Flagstaff Station[8].

[7] The APS databases can be accessed at http://aps.umn.edu.
[8] See http://www.nofs.navy.mil/data/fchpix/.

REFERENCES

Boisson, C., Joly, M., Moultaka, J., Pelat, D., & Serote Roos, M. 2000, A&A, 357, 850
Bothun, G., & Cornell, M. 1990, AJ, 99, 1004
Cid Fernandes, R., Heckman, T., Schmitt, H., Delgado, R. M. G., & Storchi-Bergmann, T. 2001, ApJ, 558, 81
Corbett, E. A., et al. 2003, ApJ, 583, 670
Coziol, R., Torres, C. A. O., Quast, G. R., Contini, T., & Davoust, E. 1998, ApJS, 119, 239
da Costa, L. N., et al. 1994, ApJ, 424, L1
———. 1998, AJ, 116, 1
de Grijp, M. H. K., Lub, J., & Miley, G. K. 1987, A&AS, 70, 95
Dultzin-Hacyan, D., Krongold, Y., Fuentes-Guridi, I., & Marziani, P. 1999, ApJ, 513, L111
González Delgado, R. M., Heckman, T., & Leitherer, C. 2001, ApJ, 546, 845
Gu, Q., Dultzin-Hacyan, D., & de Diego, J. A. 2001, Rev. Mex. AA, 37, 3
Hernández Toledo, H. M., Dultzin-Hacyan, D., & Sulentic, J. W. 2001, AJ, 121, 1319
Ho, L. C. 2005, preprint (astro-ph/0511157)
Ho, L. C., Filippenko, A. V., & Sargent, W. L. 1995, ApJS, 98, 477
Huchra, J. 1990, Center for Astrophysics Redshift Catalog (Cambridge: CfA)
Hunt, L. K., & Malkan, M. A. 1999, ApJ, 516, 660
Kauffmann, G., et al. 2003, MNRAS, 346, 1055
Kim, M., Ho, L. C., & Im, M. 2006, ApJ, 642, 702
Koulouridis, E., Plionis, M., Chavushyan, V., Dultzin-Hacyan, D., Krongold, Y., & Goudis, C. 2006, ApJ, 639, 37
Krongold, Y., Dultzin-Hacyan, D., & Marziani, P. 2002, ApJ, 572, 169
Krongold, Y., Dultzin-Hacyan, D., Marziani, P., & de Diego, J. A. 2003, Rev. Mex. AA, 39, 225
Marzke, R. O., Huchra, J. P., & Geller, M. J. 1994, ApJ, 428, 43
Mirabel, I. F., & Sanders, D. B. 1988, ApJ, 335, 104
Nicastro, F. 2000, ApJ, 530, L65
Oliva, E., Origlia, L., Maiolino, R., & Moorwood, A. F. M. 1999, A&A, 350, 9
Sanders, D. B., Egami, E., Lipari, S., Mirabel, I. F., & Soifer, B. T. 1995, AJ, 110, 1993
Sanders, D. B., Mazzarella, J. M., Kim, D.-C., Surace, J. A., & Soifer, B. T. 2003, AJ, 126, 1607
Sanders, D. B., Surace, J. A., & Ishida, C. M. 1999, in IAU Symp. 186, Galaxy Interactions at Low and High Redshift, ed. J. E. Barnes & D. B. Sanders (Dordrecht: Kluwer), 289
Serber, W., Bahcall, N., Menard, B., & Richards, G. 2006, ApJ, 643, 68
Siebenmorgen, R., Haas, M., Krügel, E., & Schulz, B. 2005, A&A, 436, L5
Soifer, B. T., Boehmer, L., Neugebauer, G., & Sanders, D. B. 1989, AJ, 98, 766
Surace, J. A., Sanders, D. B., & Mazzarella, J. M. 2004, AJ, 127, 3235
Tran, H. D. 2003, ApJ, 583, 632
Veilleux, S., Goodrich, R. W., & Hill, G. J. 1997, ApJ, 477, 631
Wang, J. L., Xia, X. Y., Mao, S., Cao, C., Wu, H., & Deng, Z. G. 2006, ApJ, 649, 722
Willmer, C. N. A., da Costa, L. N., & Pellegrini, P. S. 1998, AJ, 115, 869
Zickgraf, F.-J., Voges, W., Krautter, J., Thiering, I., Appenzeller, I., Mujica, R., & Serrano, A. 1997, A&A, 323, L21